DOI: 10.1002/chem.201001367

Bionanoprobes with Excellent Two-Photon-Sensitized Eu^{3+} Luminescence Properties for Live Cell Imaging

Guangsheng Shao,[a] Rongcheng Han,[a] Yan Ma,[a] Minxian Tang,[a] Fumin Xue,[a] Yinlin Sha,[b] and Yuan Wang*[a]

Bioimaging or bioanalysis based on nanoprobes encapsulating Eu^{3+} complexes with excellent two-photon-sensitized (TPS) luminescence properties combines the advantages of deep penetration, high sensitivity, high signal-to-noise ratio, stable signals during long term observation, low photodamage to biological samples, and desirable target recognizability.

The TPS luminescence of lanthanide complexes is produced through the two-photon excitation (TPE) of a light-harvesting antenna ligand and subsequent excitation energy transfer (EET) to the metal ions, which provides a promising manner for extending the excitation windows of lanthanide complexes to the near-infrared (NIR) light wavelength region. In the last two decades, remarkable progress has been achieved in the design and synthesis of two-photon-sensitized luminescent lanthanide complexes.[1] Several lanthanide complexes have been applied to the multiphoton-excited bioimaging of cells.[2–4] Due to the characteristic luminescence properties of Eu^{3+} complexes, such as the characteristic narrow-line emission in the red-light wavelength region with acceptable transparence for many biosamples, high luminescence quantum yields, large Stokes shifts, and long luminescence lifetime (millisecond order), the TPS Eu^{3+} luminescence is of significance for developing bioanalysis or bioimaging technologies.

[a] G. Shao,[+] Dr. R. Han,[+] Dr. Y. Ma, M. Tang, F. Xue, Prof. Y. Wang
Beijing National Laboratory for Molecular Sciences
State Key Laboratory for Structural Chemistry of Unstable and Stable Species, College of Chemistry and Molecular Engineering
Peking University, Beijing 100871 (P.R. China)
Fax: (+86) 10-6276-5769
E-mail: wangy@pku.edu.cn

[b] Prof. Y. Sha
Department of Biophysics, School of Basic Medical Sciences and Biomed-X Center, Peking University, Beijing 100191 (P.R. China)

[+] These authors contributed equally to this work.

Supporting information for this article is available on the WWW under http://dx.doi.org/10.1002/chem.201001367.

In comparison with free Eu^{3+} complex molecules, nanoprobes encapsulating luminescent Eu^{3+} complexes possess the additional benefits of remarkably enhanced brightness, chemical stability, and photostability, since each nanoparticle contains a lot of complex molecules shielded by a matrix.[5] However, reports on bionanoprobes encapsulating europium complexes that can be efficiently two-photon excited by NIR laser irradiation have so far been scarce.

In the past few years, we reported an interesting complex $[Eu(tta)_3dpbt]$ (tta = thenoyltrifluoroacetonato, dpbt = 2-(*N*,*N*-diethylanilin-4-yl)-4,6-bis-(3,5-dimethylpyrazol-1-yl)-1,3,5-triazine) (see the Supporting Information, Scheme S1) and its derivatives, which exhibit efficiently visible-light-sensitized and two-photon-sensitized Eu^{3+} luminescence with action cross sections ($\delta \times \Phi$) of 82–85 GM (1 GM = 10^{-50} cm^4 s photon^{-1} molecule^{-1}) at 808–812 nm.[6,7] The excitation energy transfer from dpbt to Eu^{3+} in $[Eu(tta)_3dpbt]$ is dominated by a singlet energy-transfer pathway.[6,7d] $[Eu(tta)_3dpbt]$ nanoparticles protected by cetyltrimethyl ammonium bromide (CTAB) in water/methanol mixtures exhibited excellent visible-light-sensitized and two-photon-sensitized luminescence properties with a $\delta \times \Phi$ value of 3.2×10^5 GM (1 GM = 10^{-50} cm^4 s photon^{-1} particle^{-1}) at 832 nm.[8] These results encouraged us to make efforts to encapsulate $[Eu(tta)_3dpbt]$ in water-dispersible nanoparticles for the preparation of bioprobes applicable in two-photon-excitation bioimaging or bioanalysis. However, the simple use of $[Eu(tta)_3dpbt]$ in the preparation of such luminescent nanoparticles with conventional microemulsion polymerization or Stöber method[9] resulted in the loss of its luminescent properties because of the reactions between the complex and compounds appearing in these processes.

Herein, we report novel nanospheres (EuLNPs), characterized by encapsulation of $[Eu(tta)_3dpbt]$ in the hydrophobic cores of water-dispersible and biocompatible nanoparticles of poly(methyl methacrylate-*co*-methacrylic acid) (PMMA-*co*-MAA). These nanospheres exhibited excellent TPS Eu^{3+} luminescence properties ($\delta \times \Phi$ 1.2×10^5 GM at 825 nm, 1 GM = 10^{-50} cm^4 s photon^{-1} particle^{-1}) and high dis-

persion stability in water solutions. As tractable building blocks, EuLNPs were conjugated with anti-epidermal growth factor receptor monoclonal antibody (anti-EGFR) to form bionanoprobes (antiEGFR@EuLNPs), which were successfully applied in the TPE cell-selective imaging of live cancer cells.

A stable colloidal solution of EuLNPs in water was prepared easily by adding an acetone solution containing [Eu(tta)$_3$dpbt] and PMMA-*co*-MAA to pure water and the treatment processes described in the Experimental Section. Due to the potential applications ranging from controlled release to rheological modifications, the micellization behavior of the block copolymer poly(methyl methacrylate-*block*-methacrylic acid) (PMMA-*b*-MAA) and its core shell-like micelles in aqueous medium have been well studied.[10] However, reports on the water dispersible nanoparticles of the random copolymer PMMA-*co*-MAA have so far been scarce. Both PMMA-*co*-MAA and [Eu(tta)$_3$dpbt] are insoluble in water. When an acetone solution containing [Eu(tta)$_3$dpbt] and PMMA-*co*-MAA was added to water, coprecipitation and assembly of these compounds occurred to form the present colloidal nanoparticles, accompanied by the encapsulation of [Eu(tta)$_3$dpbt] in the hydrophobic cores and exposing a part of the carboxyl groups to water.

EuLNPs in the prepared hydrosol were separated by centrifugation as a precipitate which was redispersed in PBS–BSA (phosphate buffered saline (PBS, pH 7.4) solution containing 1.0 g L^{-1} bovine serum albumin (BSA)) to form a colloidal solution. No precipitate was observed after the prepared colloidal solutions were stored under ambient conditions for months, suggesting the excellent dispersion stability of EuLNPs in water and PBS–BSA.

The zeta potential of the EuLNPs dispersed in pure water was measured to be -18.0 ± 1.5 mV, which was derived from the ionization of the carboxyl groups at the surfaces of the EuLNPs. The hydrodynamic diameter of the EuLNPs was measured by dynamic light scattering (DLS) at 25 °C to be 62 nm. Figure 1 shows the TEM image and size distributions of the EuLNPs in the hydrosol. The EuLNPs prepared in this work are spherical in shape with an average diameter of 52 nm. The difference between the average sizes measured by DLS and TEM in this work should be mainly derived from the bigger contribution to the light scattering signals of the large particles in the sample than the small ones.

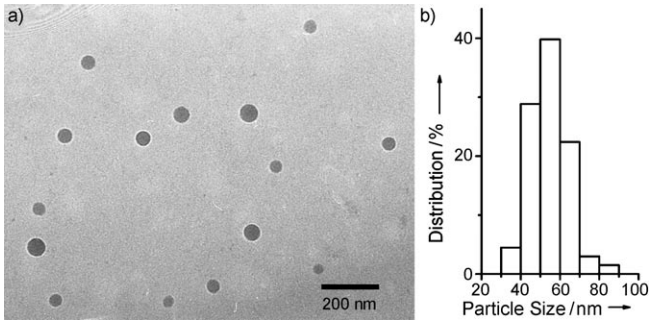

Figure 1. TEM image (a) and the size distributions (b) of EuLNPs with an average diameter of 52 nm.

Figure 2 shows the UV/Vis absorption spectrum, luminescence excitation spectrum, photoluminescence spectrum and two-photon excitation action cross sections of a colloidal solution of EuLNPs in PBS–BSA. As shown in Figure 2a, the UV/Vis absorption spectrum of EuLNPs in the colloidal so-

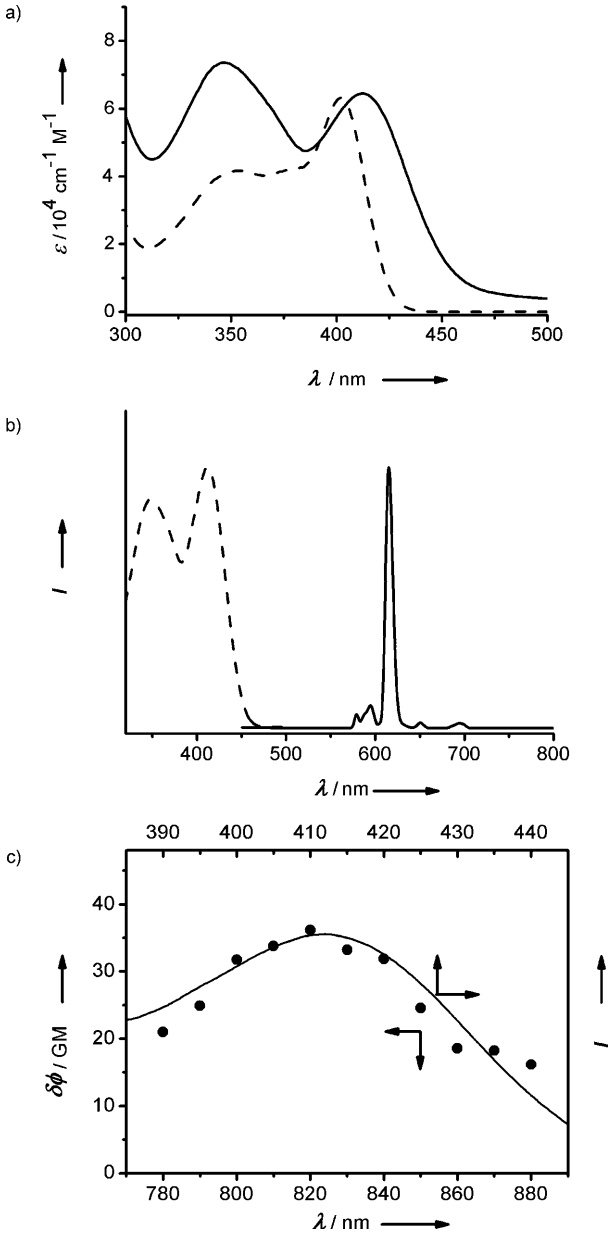

Figure 2. a) UV/Vis absorption spectra of the EuLNPs in colloidal solution (solid line) and [Eu(tta)$_3$dpbt] dissolved in toluene (dashed line); b) Normalized luminescence excitation spectrum (dashed line, $\lambda_{em}=614$ nm) and photoluminescence spectrum (solid line, $\lambda_{ex}=412$ nm) of the EuLNPs in colloidal solution; c) Two-photon excitation action cross sections ($\delta\times\Phi$) (●) and one-photon excitation spectrum ($\lambda_{em}=614$ nm) (solid line) for the EuLNPs in colloidal solution (1 GM = 10^{-50} cm^4 s photon^{-1} molecule^{-1}, the experimental uncertainty for $\delta\times\Phi$ is about 15 %.). Colloidal EuLNPs dispersed in PBS–BSA were used in these measurements.

lution shows a maximal absorption peak in the visible-light wavelength region centered at 412 nm originating from the coordinated dpbt ligand, whereas the corresponding absorption band of [Eu(tta)$_3$dpbt] dissolved in toluene is located at 402 nm. The maximal molar extinction coefficient (ε) of [Eu(tta)$_3$dpbt] molecules in the EuLNPs colloidal solution was estimated to be $6.5\times10^4\,\text{M}^{-1}\,\text{cm}^{-1}$ at 412 nm, which was approximate to that of [Eu(tta)$_3$dpbt] dissolved in toluene at 402 nm ($\varepsilon_{402\text{ nm}}=6.3\times10^4\,\text{M}^{-1}\,\text{cm}^{-1}$).[7c]

As shown in Figure 2b, EuLNPs exhibited a wide excitation window for europium luminescence with a maximal excitation band at 412 nm and a red edge extending up to 475 nm, which red shifted by 10 and 35 nm relative to those of [Eu(tta)$_3$dpbt] dissolved in toluene, respectively.[6] The intensity of the absorption band at 350 nm is stronger than that at 412 nm, whereas the excitation band intensity at 350 nm is lower than that at 412 nm, indicating that the quantum yield of the Eu^{3+} luminescence of EuLNPs under UV excitation at 350 nm is less than that upon excitation with visible light at 412 nm (see the Supporting Information, Figure S1).

The decay curve of europium luminescence at 614 nm ($\lambda_{ex}=412$ nm) corresponding to the $^5D_0\rightarrow{}^7F_2$ transition of Eu^{3+} in [Eu(tta)$_3$dpbt] could be well accounted for by a two exponential-decay model function (see the Supporting Information, Figure S2), giving two apparent decay time constants of 586 μs (80%) and 158 μs (20%). The phenomena of excitation-window red shift and multiple decay time constants have been observed in the previously reported CTAB-protected [Eu(tta)$_3$dpbt] nanoparticles, which was attributed to the formation of J-type molecular aggregates of [Eu(tta)$_3$dpbt] in the particles.[8] The photostability of EuLNPs was measured by using a 150 W xenon lamp as an excitation source. The emission intensity decreased by only 8% after irradiation for 1 h, indicating the good photostability of EuLNPs (see the Supporting Information, Figure S3).

The luminescence quantum yield (Φ) for the Eu^{3+} emission of EuLNPs was measured to be 0.31 at 412 nm at 20°C with 4-dicyanomethylene-2-methyl-6-*p*-dimethylaminostyryl-4H-pyran in *n*-propanol as the reference ($\Phi=0.57$).[11] In the calculation of the luminescence quantum yield of prepared nanoparticles, the influence of scattering intensity was not removed, that is, the luminescence quantum yield of [Eu(tta)$_3$dpbt] in EuLNPs is higher than that of the nanoparticles. Assuming that the density of EuLNPs is about $1.1\,\text{g}\,\text{cm}^{-3}$ (the densities of PMMA-*co*-MAA and [Eu(tta)$_3$dpbt] are 1.16 and $0.92\,\text{g}\,\text{cm}^{-3}$, respectively), it can be estimated that each nanosphere with the average diameter ($d_{av}=52$ nm) contains about 3500 [Eu(tta)$_3$dpbt] molecules (see the Supporting Information for details). The luminescent brightness of EuLNPs (defined as $\varepsilon\times\Phi$) is estimated to be $7.0\times10^7\,\text{M}^{-1}\,\text{cm}^{-1}$ under excitation at 412 nm at 20°C, suggesting a remarkable signal amplification capability of EuLNPs in bioanaylsis.

As shown in Figure 2c, the maximal TPE action cross section ($\delta\times\Phi$) of [Eu(tta)$_3$dpbt] molecules in EuLNPs was measured to be 35 GM at 20°C ($\lambda_{ex}=825$ nm, 1 GM = $10^{-50}\,\text{cm}^4\,\text{s}\,\text{photon}^{-1}\,\text{molecule}^{-1}$) with rhodamine B in methanol as the reference,[12] which was approximate to that in the CTAB-protected [Eu(tta)$_3$dpbt] nanoparticles ($\delta\times\Phi_{832\text{ nm}}=37.4$ GM).[8] Since each nanoparticle with the average size contains about 3500 [Eu(tta)$_3$dpbt] molecules, the maximal TPE action cross section of EuLNPs ($d_{av}=52$ nm) is estimated to be 1.2×10^5 GM (1 GM = $10^{-50}\,\text{cm}^4\,\text{s}\,\text{photon}^{-1}\,\text{particle}^{-1}$). This $\delta\times\Phi$ value is twice as much as that of CdSe/ZnS core-shell quantum dots ($d_{av}=4.5$ nm) determined by a similar method.[13] The high $\delta\times\Phi$ value and the characteristic Eu^{3+} emission enables EuLNPs to be promising luminescence emitters for bionanoprobes in TPE imaging applications.

For practical applications, a luminescent bioprobe should not interfere with the metabolism of the living system. Cytotoxicity tests were performed with HeLa and Lewis carcinoma cells by the methyl thiazolyl tetrazolium (MTT) assay (see the Supporting Information for details).[14] The living cells were exposed to buffer solutions with different concentrations of EuLNPs for 12 h, and the percentages of the viable cells were quantified. No apparent cytotoxicity was observed to HeLa and Lewis cells even when the concentration of EuLNPs was increased up to $100.0\,\mu\text{g}\,\text{mL}^{-1}$ (7.4 μM [Eu(tta)$_3$dpbt]) (see the Supporting Information, Figure S4). The cytotoxicity of EuLNPs is much lower than that of the complex [Eu(tta)$_2$Cldpbt] which killed 30% HeLa cells when the concentration of [Eu(tta)$_2$Cldpbt] was $1.0\,\mu\text{g}\,\text{mL}^{-1}$ (0.9 μM).[3] The high biocompatibility of PMMA-*co*-MAA and the efficient shielding of [Eu(tta)$_3$dpbt] molecules by the matrix in EuLNPs may be a cause of the low cytotoxicity of EuLNPs to the cells.

Epidermal growth factor receptor (EGFR), over-expressed in many cancer types, provides an opportunity for designing receptor-targeted approaches for cancer detection and treatment. Previous studies have examined the feasibility of conjugating nanoparticles with an anti-EGFR monoclonal antibody.[15] In this work, anti-EGFR monoclonal antibodies were anchored on the surfaces of EuLNPs to form bionanoprobes (antiEGFR@EuLNPs) by the EDC/Sulfo-NHS (EDC = 1-ethyl-3-(3-dimethylaminopropyl) carbodiimide hydrochloride, Sulfo-NHS = *N*-hydroxysulfosuccinimide sodium salt) chemical conjugating strategy, which allows the exposed carboxyl groups at the surface of the EuLNPs to conjugate with the amino groups of anti-EGFR (see the Supporting Information, Scheme S2).

Figure 3 shows the TPE luminescence images of MDA-MB-231 cells incubated for 3 h at 37°C in the presence of antiEGFR@EuLNPs. As shown in Figure 3a, strong red luminescence signals were detected in the MDA-MB-231 cells, which express a high level of EGFR. A comparison of Figure 3a with the phase contrast image (Figure 3b) clearly indicated that antiEGFR@EuLNPs efficiently labeled MDA-MB-231 cells (Figure 3c). In contrast, the Eu^{3+} luminescence signal cannot be observed in a negative control experiment under the same experimental conditions with MCF-7 cells that have a low level of EGFR (see the Supporting Information, Figure S5). These results revealed that live MDA-MB-

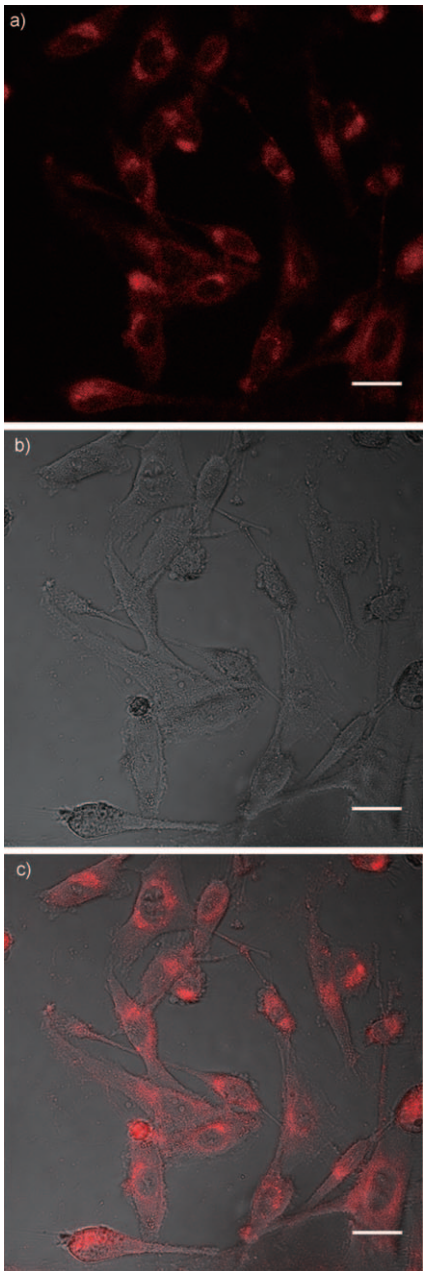

Figure 3. Images of MDA-MB-231 cells treated with antiEGFR@EuLNPs. a) Two-photon-excited luminescence images; b) Differential interference contrast (DIC) images; c) The overlay of the corresponding luminescence and DIC images. Cells were incubated with antiEGFR@EuLNPs for 3 h at 37 °C, and washed with PBS solution three times before imaging. Scale bars: 50 μm.

231 cells were receptor-targeted labeled by antiEGFR@EuLNPs. To the best of our knowledge, antiEGFR@EuLNPs is the first cancer-cell-targeted bionanoprobe encapsulating europium complexes that can be efficiently two-photon excited by NIR laser irradiation.

It should be mentioned that live cells with normal metabolism were used in our experiments. In contrast to the static and snapshot view of fixed cells,[4] live cell imaging can provide more vital information about interactions within and among cells as they grow and differentiate, which will be helpful for understanding the cell functions.

In summary, [Eu(tta)dpbt] was efficiently encapsulated in water-dispersible nanospheres of PMMA-*co*-MAA with an average diameter of 52 nm by the proposed coprecipitation–assembly method developed in this work. The prepared nanospheres exhibited desirable two-photon-sensitized luminescence properties with a $\delta \times \Phi$ value of 1.2×10^5 GM ($1\ \mathrm{GM} = 10^{-50}\ \mathrm{cm^4\,s\,photon^{-1}\,particle^{-1}}$), high dispersion stability in water solutions, high photostability, and excellent biocompatibility. An anti-EGFR monoclonal antibody was anchored on the surfaces of EuLNPs to form the bionanoprobes antiEGFR@EuLNPs. The target-specific two-photon-excitation imaging of live MDA-MB-231 cancer cells was realized with antiEGFR@EuLNPs as the bionanoprobe. Further study on the live animal imaging based on such bionanoprobes is ongoing within our group.

Experimental Section

Preparation of EuLNPs: EuLNPs were prepared by a coprecipitation–assembly method. In a typical experiment, an acetone solution (2 mL) containing [Eu(tta)$_3$dpbt] (0.20 mg) and PMMA-*co*-MAA (2.0 mg, MW: 34000, molar proportion of methyl methacrylate to methacrylic acid is 1:0.016) was added dropwise into water (8 mL) under stirring at RT. The mixture was further stirred for about 10 min, yielding a yellow colloidal solution. Acetone in the colloidal solution was removed at 35 °C by rotary evaporation, and then the colloidal solution was heated under reflux at 100 °C for 40 min. Then the supernatant was centrifuged at 50000 g to get a precipitate of EuLNPs, which was redispersed by ultrasonic irradiation in pure water or PBS–BSA (PBS solution (pH 7.4) containing 1.0 g L^{-1} BSA) to form stable colloidal solutions of EuLNPs (8 mL).

Preparation of EuLNPs–antiEGFR nanoprobe: The obtained colloidal solution of EuLNPs in water (8 mL) was mixed with a PBS solution (0.1 mL, pH 7.4) containing EDC (10 mg) and Sulfo-NHS (10 mg), and then the mixture was incubated for 30 min at 25 °C in a Thermomix shaker (Eppendorf, Germany) at 300 rpm. After being separated by centrifugation and washed with PBS solution (pH 7.4), the resulting activated EuLNPs were dispersed in PBS solution (10 mL, pH 7.4) by ultrasonic irradiation. To this colloidal solution, an anti-EGFR monoclonal antibody solution (0.5 mg of anti-EGFR monoclonal antibody in PBS buffer, 0.1 mL) was added, and the obtained mixture was incubated for 5 h at 25 °C in the Thermomix shaker at 300 rpm. After being separated by centrifugation and washed with PBS solution (pH 7.4), the resulting anti-EGFR-functionalized EuLNPs (antiEGFR@EuLNPs) were dispersed in PBS–BSA (5 mL) by ultrasonic irradiation and stored at 4 °C.

Cell imaging: MDA-MB-231 and MCF-7 cells were propagated in RPMI Medium 1640 supplemented with 10 % fetal bovine serum (FBS) and 80 U ml^{-1} gentamycin sulfate. Then the cultured cells were trypsinized and resuspended in this RPMI Medium 1640 at a concentration of about 7.5×10^5 mL^{-1}. The cell suspension (100 μL) was transferred to a confocal dish (35 mm). After incubation for 24 h at 37 °C in 5 % CO_2, the cells were carefully rinsed with PBS solution (pH 7.4). Then a colloidal solution of antiEGFR@EuLNPs (100 μL, 0.2 g L^{-1}) was added. After incubation for 3 h at 37 °C in 5 % CO_2, the dish was rinsed three times with PBS solution (pH 7.4) and then fresh serum-free medium (1 mL) was added. The plates were incubated for another 10 min at 37 °C and then directly imaged on an upright confocal microscope (Leica TCS SP5) equipped with a femtosecond Ti:sapphire laser and a 20× water immersion objective (Carl Zeiss). The TPE luminescence images were taken upon femtosecond 783 nm irradiation ($\varepsilon \times \Phi_{783\ \mathrm{nm}} = 8.8 \times 10^4$ GM), and integration of Eu^{3+} luminescence in the spectral range of 590–620 nm. For comparison,

all of the confocal images were taken with the same setting. Transmitted light differential interference contrast (DIC) images were taken on the same instrument.

See the Supporting Information for materials, measurements, cytotoxicity experiments, Schemes S1 and S2, and Figures S1–S6.

Acknowledgements

The authors express their thanks for the joint support from the NSFC (project nos.: 50821061 and 20973003), the NKBRSF (G2006CB806102), and the 863 program (2006AA02090405) from the Chinese Ministry of Science and Technology.

Keywords: bioimaging · europium · imaging agents · luminescence · nanoparticles

[1] a) J. C. G. Bünzli, C. Piguet, *Chem. Soc. Rev.* **2005**, *34*, 1048–1077; b) S. V. Eliseeva, J. C. G. Bünzli, *Chem. Soc. Rev.* **2010**, *39*, 189–227; c) J. C. G. Bünzli, S. V. Eliseeva, *Lanthanide Spectroscopy, Materials, and Bio-applications, Vol. 7* (Ed.: P. Hänninen, H. Härmä), Springer, Berlin, **2010**, Chapter 2.

[2] a) C. Andraud, O. Maury, *Eur. J. Inorg. Chem.* **2009**, 4357–4371; b) G. L. Law, K. L. Wong, C. W. Y. Man, W. T. Wong, S. W. Tsao, M. H. W. Lam, P. K. S. Lam, *J. Am. Chem. Soc.* **2008**, *130*, 3714–3715; c) F. Kielar, A. Congreve, G. L. Law, E. J. New, D. Parker, K. L. Wong, P. Castreno, J. de Mendoza, *Chem. Commun.* **2008**, 2435–2437; d) F. Kielar, G. L. Law, E. J. New, D. Parker, *Org. Biomol. Chem.* **2008**, *6*, 2256–2258; e) S. V. Eliseeva, G. Auböck, F. van Mourik, A. Cannizzo, B. Song, E. Deiters, A. S. Chauvin, M. Chergui, J. C. G. Bünzli, *J. Phys. Chem. B* **2010**, *114*, 2932–2937.

[3] G. L. Law, K. L. Wong, C. W. Y. Man, S. W. Tsao, W. T. Wong, *J. Biophotonics* **2009**, *2*, 718–724.

[4] A. Picot, A. D'Aleo, P. L. Baldeck, A. Grichine, A. Duperray, C. Andraud, O. Maury, *J. Am. Chem. Soc.* **2008**, *130*, 1532–1533.

[5] a) S. Heer, O. Lehmann, M. Haase, H. U. Güdel, *Angew. Chem.* **2003**, *115*, 3288–3291; *Angew. Chem. Int. Ed.* **2003**, *42*, 3179–3182; b) H. S. Peng, C. F. Wu, Y. F. Jiang, S. H. Huang, J. McNeill, *Langmuir* **2007**, *23*, 1591–1595; c) F. Meiser, C. Cortez, F. Caruso, *Angew. Chem.* **2004**, *116*, 6080–6083; *Angew. Chem. Int. Ed.* **2004**, *43*, 5954–5957; d) J. Wu, Z. Q. Ye, G. L. Wang, D. Y. Jin, J. L. Yuan, Y. F. Guan, J. Piper, *J. Mater. Chem.* **2009**, *19*, 1258–1264.

[6] C. Yang, L. M. Fu, Y. Wang, J. P. Zhang, W. T. Wong, X. C. Ai, Y. F. Qiao, B. S. Zou, L. L. Gui, *Angew. Chem.* **2004**, *116*, 5120–5123; *Angew. Chem. Int. Ed.* **2004**, *43*, 5010–5013.

[7] a) L. M. Fu, X. F. Wen, X. C. Ai, Y. Sun, Y. S. Wu, J. P. Zhang, Y. Wang, *Angew. Chem.* **2005**, *117*, 757–760; *Angew. Chem. Int. Ed.* **2005**, *44*, 747–750; b) R. Hao, M. Y. Li, Y. Wang, J. P. Zhang, Y. Ma, L. M. Fu, X. F. Wen, Y. S. Wu, X. C. Ai, S. W. Zhang, Y. G. Wei, *Adv. Funct. Mater.* **2007**, *17*, 3663–3669; c) F. M. Xue, L. M. Fu, R. Hao, G. S. Shao, M. X. Tang, J. P. Zhang, Y. Wang, *Phys. Chem. Chem. Phys.* **2010**, *12*, 3195–3202; d) L. M. Fu, X. C. Ai, M. Y. Li, X. F. Wen, R. Hao, Y. S. Wu, Y. Wang, J. P. Zhang, *J. Phys. Chem. A* **2010**, *114*, 4494–4500.

[8] X. F. Wen, M. Y. Li, Y. Wang, J. P. Zhang, L. M. Fu, R. Hao, Y. Ma, X. C. Ai, *Langmuir* **2008**, *24*, 6932–6936.

[9] a) S. Santra, P. Zhang, K. M. Wang, R. Tapec, W. H. Tan, *Anal. Chem.* **2001**, *73*, 4988–4993; b) Z. Q. Ye, M. Q. Tan, G. L. Wang, J. L. Yuan, *Anal. Chem.* **2004**, *76*, 513–518; c) K. L. Ai, B. H. Zhang, L. H. Lu, *Angew. Chem.* **2009**, *121*, 310–314; *Angew. Chem. Int. Ed.* **2009**, *48*, 304–308.

[10] J. Yao, P. Ravi, K. C. Tam, L. H. Gan, *Langmuir* **2004**, *20*, 2157–2163.

[11] J. N. Demas, G. A. Crosby, *J. Phys. Chem.* **1971**, *75*, 991–1024.

[12] C. Xu, W. W. Webb, *J. Opt. Soc. Am. B* **1996**, *13*, 481–491.

[13] D. R. Larson, W. R. Zipfel, R. M. Williams, S. W. Clark, M. P. Bruchez, F. W. Wise, W. W. Webb, *Science* **2003**, *300*, 1434–1436.

[14] R. C. Han, M. Yu, Q. Zheng, L. J. Wang, Y. K. Hong, Y. L. Sha, *Langmuir* **2009**, *25*, 12250–12255.

[15] a) I. H. El-Sayed, X. H. Huang, M. A. El-Sayed, *Cancer Lett.* **2006**, *239*, 129–135; b) I. H. El-Sayed, X. H. Huang, M. A. El-Sayed, *Nano Lett.* **2005**, *5*, 829–834; c) K. Sokolov, M. Follen, J. Aaron, I. Pavlova, A. Malpica, R. Lotan, R. Richards-Kortum, *Cancer Res.* **2003**, *63*, 1999–2004; d) L. L. Yang, H. Mao, Y. A. Wang, Z. H. Cao, X. H. Peng, X. X. Wang, H. W. Duan, C. C. Ni, Q. G. Yuan, G. Adams, M. Q. Smith, W. C. Wood, X. H. Gao, S. M. Nie, *Small* **2009**, *5*, 235–243.

Received: May 19, 2010
Published online: June 25, 2010

